CST Simulations of Dark Radio Experiment

Nathaniel MacFadden*
Reed College and
UC Davis

Mentor: Mani Tripathi† and Mentor: Tony Tyson‡
UC Davis
(Dated: October 8, 2018)

This paper presents a calculation of the effective in situ antenna factor of an arbitrary antenna using simulation software CST. This work is focused on the 'Dark Radio' dark matter search and thus focuses on simulating the feed voltage of an antenna in a Faraday cage excited by dark photons. Electrical and physical modeling of the surroundings and antenna were performed showing agreement to expectations, but more benchmarking should be done. Additionally, an excitation method was developed to emulate dark photon fields. This results in an antenna factor that can be used to determine the coupling, ϵ, from feed voltage.

I. INTRODUCTION

The nature of dark matter is one of the biggest open problems in physics. At a high level, our theory of gravitation has been well tested and verified in high acceleration regions (e.g., the Earth, our solar system) but observations in low acceleration regions (e.g., galaxies and galaxy clusters) deviate from predictions. This discrepancy is old, with modern investigation beginning with Lord Kelvin's lecture in 1904 [11], yet it is still unanswered.

There are three possible resolutions to this discrepancy: our observations are faulty, our understanding of dynamics is flawed, or our observations are correct but there is unobserved mass ('dark matter'). Improved observations have made the first option unlikely and thus the discrepancy exists and is either in faulty dynamics or dark matter. These options are discussed in detail in appendix A 3 but, to summarize, modifications to dynamics have been unable to explain galaxy cluster observations and thus dark matter is the most promising avenue.

While many dark matter theories are losing parameter space with each generation of experiments, this paper focuses on a relatively unexplored dark matter theory: 'dark photons'. See figure 1 for an overview of the available dark matter parameter space and what is constraining it. This plot shows a large area of interest for dark photons ('hidden photino'), a large motivation for their current search.

Technically, dark photons are hypothesized low mass vector bosons that interact with the standard model via kinetic mixing. They are described by new massive vector fields that can be thought of as a copy of electromagnetism with minor differences to be discussed in section II. This theory is discussed in more detail in appendix B but the details of that discussion are not needed for this work.

II. THEORY

Light is a traveling excitation of electromagnetic fields whose motion is described by the wave equation:

$$\Box A^\mu = -\mu_0 J^\mu \tag{1}$$

(see appendix A for variable definitions and conventions). This equation is effectively equivalent to Maxwell's equations in their standard differential form:

$$\begin{aligned}
\nabla \cdot \mathbf{E} &= \frac{\rho_e}{\epsilon_0} && \text{Gauss's Law,}\\
\nabla \cdot \mathbf{B} &= \mu_0 \rho_m && \text{Gauss's Law for magnetism,}\\
-\nabla \times \mathbf{E} &= \frac{\partial \mathbf{B}}{\partial t} + \mu_0 \mathbf{j_m} && \text{Maxwell-Faraday eq., and}\\
\nabla \times \mathbf{B} &= \mu_0 \epsilon_0 \frac{\partial \mathbf{E}}{\partial t} + \epsilon_0 \mathbf{j}_e && \text{Ampère's circuital law,}
\end{aligned} \tag{2}$$

except that it lends itself to more advanced analysis.

An alternative and modern description of light is as a massless particle traveling at $c \equiv 299792458$ m/s in a vacuum. We call this particle a 'photon' and give it energy proportional to the frequency of traveling wave that it corresponds to. These theories are unified in QFT in which this particle is a quantized excitation of the electromagnetic fields.

In a theoretical leap, new 'dark' fields are hypothesized that are analogs of the electromagnetic fields except they are massive[14] (mass m) and their interaction with charges is suppressed (coupling ϵ). Then, just as photons are quantized excitations of electromagnetic fields, dark photons are quantized excitations of the dark fields. These modifications are clear in the wave equation describing dark fields[8]:

$$(\Box - m^2) A'^\mu = -\epsilon \mu_0 J^\mu. \tag{3}$$

* macfaddn@reed.edu
† http://tripathi.physics.ucdavis.edu/
‡ http://tyson.ucdavis.edu/

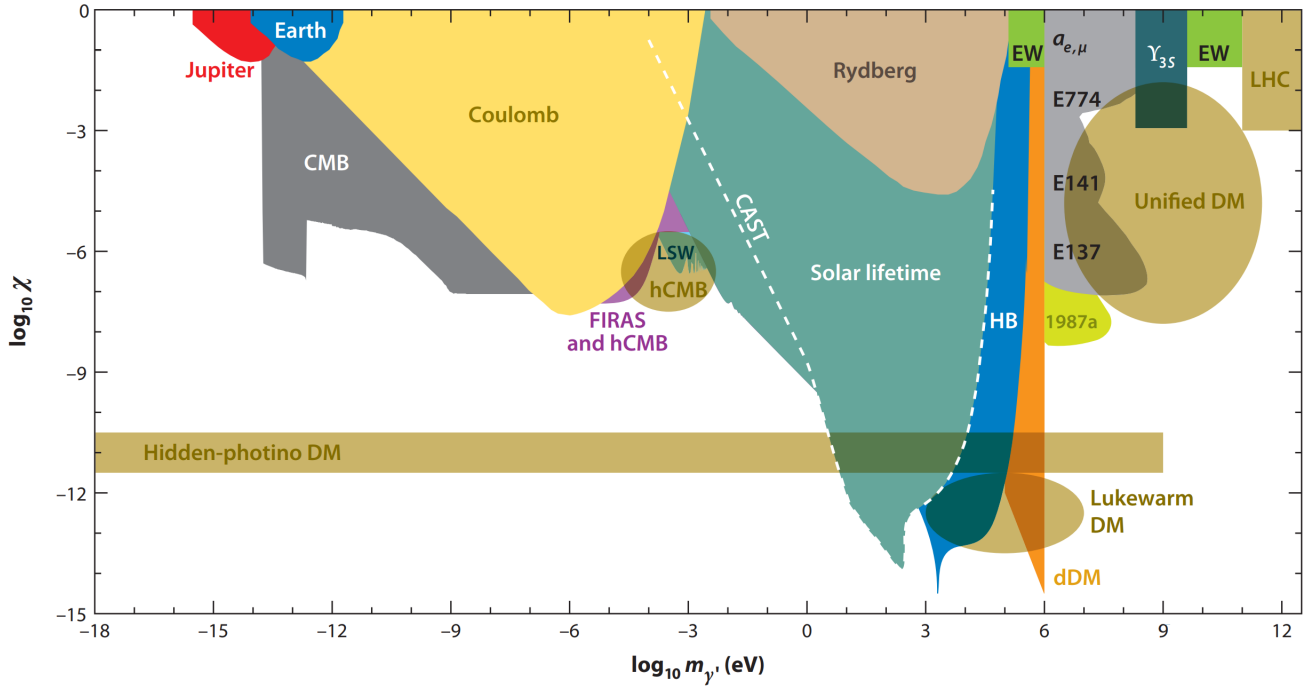

FIG. 1. (taken from [10]) Dark matter parameter space of kinetic mixing χ (ϵ in this writeup) to mass $m_{\gamma'}$ (m in this writeup). Transparent tan regions indicate areas of interest for various dark matter theories; opaque colored regions exclude dark matter.

The three dark photon parameters, then, are the field strength E' (linked to B'), mass m, and coupling ϵ.

A. Field Strength

Relativistically, mass and energy are equivalent ($E^2 = (pc)^2 + (mc^2)^2$) and thus the observational discrepancies motivating dark matter are energy discrepancies. The need for dark matter, then, is a need for a bound energy density in galaxies and galaxy clusters that has so far been unseen[15].

To see if dark photons could provide such energy density, we determine the energy density of a dark photon field known amplitude. Given a field described by Lagrangian density $\mathcal{L}$, the Hamiltonian $\mathcal{H}$ gives the energy density[16]. For electromagnetism, for example, the energy density is:

$$\mathcal{H} = \frac{1}{2\mu_0}\left(\frac{E^2}{c^2} + B^2\right) \tag{4}$$

where the Legendre transform to get the Hamiltonian is more complicated than just $\mathcal{H} = \frac{\partial \mathcal{L}}{\partial \dot{A}_\nu}\dot{A}_\nu - \mathcal{L}$ since the Hamiltonian must be gauge-independent. Performing the same Legendre transform for the dark fields results in $\mathcal{H} \approx \epsilon_0 E'^2/2$ since the B' component is velocity suppressed ($B' \propto vE'$ where v is the speed of dark matter[3]) and v small.

With the energy density of dark fields, the dark field strength can be calculated:

$$E' \approx \sqrt{2\rho_{DM}/\epsilon_0} \approx 3300\text{V/m} \tag{5}$$

using the observed local dark matter density $\rho_{DM} = 0.3 \pm 0.1$ GeV cm^{-3}[2] and assuming all dark matter is dark photons. In reality, even if dark photons are the primary dark matter component, not all of dark matter will be dark photons. The corrections by other dark matter components, however, are a finer detail than of current concern.

B. Mass and Momentum Distribution

Photons and dark photons are discrete excitations of the electromagnetic and dark fields respectively. These excitations act as quantum harmonic oscillators at every point in space and thus, the energy levels for a given frequency are separated by $h\nu$ for these oscillators, thus giving the energy of the particle $\mathcal{E} = h\nu$.

On the other hand, Einstein's energy momentum relationship gives the energy of a particle in terms of momentum and mass:

$$\mathcal{E} = \sqrt{(pc)^2 + (mc^2)^2}. \tag{6}$$

These two views combine to give the relationship: $h\nu = \sqrt{(pc)^2 + (mc^2)^2}$. For photons this simplifies to $p = h\nu/c$ since photons are massless. For dark photons, conversely, this relationship is $\nu \approx mc^2/h$ since $p \ll mc$ by looking

at momentum distributions of dark matter. Thus the frequency of any dark photon signal gives the mass m.

Despite $p \ll mc$, the dark matter momentum spread is nonzero and this does affect the observed signal. Were dark photons all without momentum, then the observed signal would be at a single frequency $\nu_{\text{signal}} = mc^2/h$ with no spread. The nonzero momentum distribution, however, acts to spread the frequency of the signal[4]:

$$\frac{mc^2}{h} \leq \nu_{\text{signal}} \lesssim \frac{mc^2}{h}(1 + 10^{-6}) \tag{7}$$

giving

$$\Delta\nu_{\text{signal}}(\nu) \sim 10^{-6}\nu \tag{8}$$

and thus a quality factor of the signal of

$$Q = \frac{\nu_{\text{signal}}(\nu)}{\Delta\nu_{\text{signal}}(\nu)} \approx 10^6. \tag{9}$$

This provides a serious constraint on possible dark photon signals: they must have a very large quality factor. Given the high probability of systematic noise entering into detectors, constraints such as this are valuable in providing confidence that a measured signal is actually from dark photons.

C. Coupling

As described in section B 3, the dark photon field interacts with charges like the electromagnetic field, except suppressed by ϵ. In other words, a field E' is equivalent to an electric field by $E = \epsilon E'$. This allows search for dark photons through electromagnetic field detectors such as antennae, which is used in this paper.

The search for dark photons is drastically different than that for high mass particles: low mass searches for weak signals through use of resonating structures; high mass searches for rare events through use of large detection volume. An example of the high mass search is LZ: a cutting edge liquid xenon time projection chamber searching for WIMPs through waiting for WIMPs to interact with xenon nuclei and produce light[1]. Both detectors need to run for long times, but for different reasons. Dark photon searches need the dark photon signal to 'ring up' while other (noisy) signals average out; WIMP searches wait until the rare event (WIMP hitting a nucleus) occurs.

The relationship between dark field strength and outputted signal must be determined. For antennae in free space, this relationship is called antenna factor and is sensitive to antenna geometry and readout electronics[17]. The antenna factor has units of inverse length and measures the electric field generated by an antenna fed an excitation voltage of 1 V.

Conducting surroundings modify the feed voltage for a given field strength and thus, in the actual calculation the detailed geometry of the room must be considered. The complexity of the geometry, especially in the actual experimental setup, requires numerical simulation to find such an (effective[18] since we take surroundings into account) antenna factor.

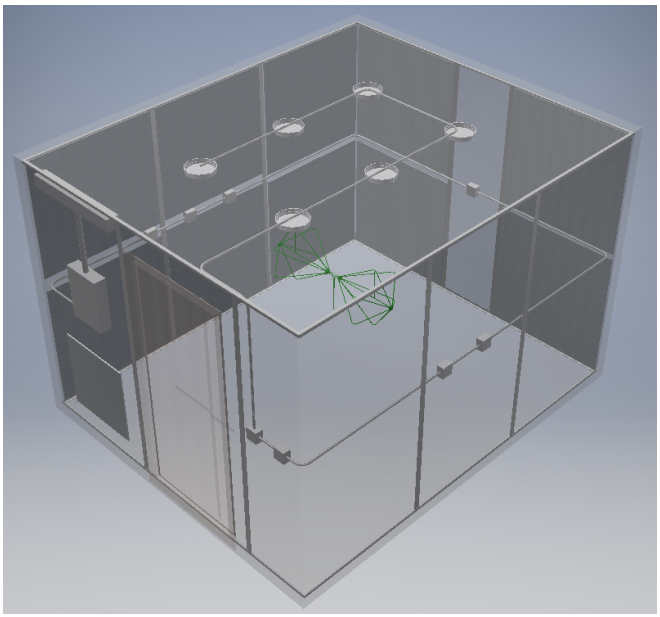

FIG. 2. CAD model of dark radio experiment. Green highlighted object in the center of the room is the bicon antenna with transmission line feed.

Defining the (effective) antenna factor as the ratio of field strength (without the antenna there) to feed voltage (with the antenna there):

$$AF(\nu) = \left|\frac{E(\nu)}{V(\nu)}\right|, \tag{10}$$

we see that knowledge of the (effective) antenna factor and feed voltage would give the coupling by:

$$\epsilon = \frac{E(\nu)}{E'(\nu)} = \frac{AF(\nu)\cdot V(\nu)}{E'(\nu)} \approx \frac{AF(\nu)\cdot V(\nu)}{3300\text{V/m}}. \tag{11}$$

Thus the antenna factor gives the coupling, the last unknown.

III. EXPERIMENTAL SETUP

A COM-POWER AB-900A biconical antenna (or 'bicon') rated for 30-300 MHz is used to measure the dark photon signal since the dark photon field is equivalent to an electric field of strength $E = \epsilon E'$. The antenna picks up other signals (e.g., wi-fi, cellular), too, and these must be canceled for accurate measurement of dark photons.

Faraday cages block electric fields through surface currents and thus are a natural solution to the ambient electromagnetic field problem. Since dark fields only interact

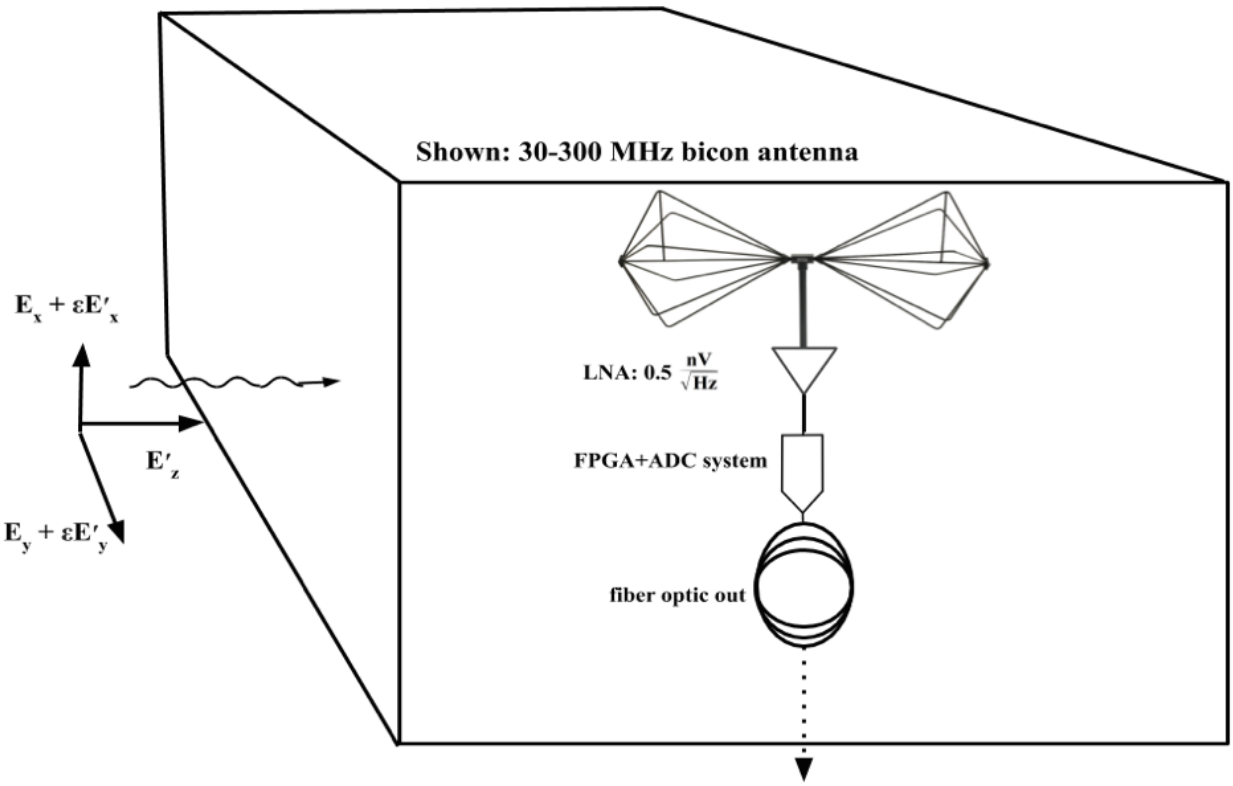

FIG. 3. Dark radio experimental schematic. Assuming dark fields propagating in the z direction, a bicon antenna (rated for 30-300MHz) is placed in the Faraday cage aligned for maximum detection efficiency. Electronics such as a balun, amplifier, and ADC are in the room before a fiber optic feed to the spectrum analyzer outside the room.

with charges very weakly (if ϵ was large, it would have already been noticed), they penetrate much deeper than electromagnetic fields. Thus, by placing the bicon inside a ETS-LINDGREN $8 \times 10 \times 12$ft Faraday cage (see figure 2), the only measurable signals should be from dark photons. More detailed discussion is provided in [8].

To measure the antenna feed signals, a Rigol RSA5065 spectrum analyzer is attached to the feed through fiber optic connections to measure the voltage across a frequency range (30-300 MHz for first tests; see figure 3). The feed voltage is monitored for extended periods of time (up to 1 year) so that noise is averaged to low levels, hopefully revealing a (weak) dark photon signal of $Q \approx 10^6$ with frequency giving m and signal strength giving ϵ. Upgrades to the electronics have been developed and are currently being tested/manufactured.

IV. SIMULATIONS

Due to the complexity of the antenna and Faraday cage, a computer simulation is needed to the effective antenna factor. In this writeup, we use CST (Computer Simulation Technology) software, which is an electromagnetic software modeling Maxwell's equations. While dark photons modify Maxwell's equations, the antenna measures the electromagnetic fields that the dark fields create and thus this software is sufficient.

There are three main tasks involved in this simulation:

1. determine excitation method to simulate dark fields,
2. model and benchmark the experiment, and
3. simulate the (effective) antenna factor.

These simulations are a non-standard use-case of CST, making verification even more important than normal.

A. Wall Currents

As shown in [8], the dark fields are found to be equivalent to AC surface currents $E \propto J\nu$ in the walls of the Faraday cage (E the real electric field generated by dark photons and J the surface currents on the walls of the waveguide) polarized in the same direction of the dark photon field. For these simulations the frequencies of interest are $\nu \in [30, 300]$ MHz and the dark fields are assumed to be polarized along the antenna axis. These currents are induced using the tool 'Field Source' and they excite a field inside the cage that is propagated by CST's numerical solver.

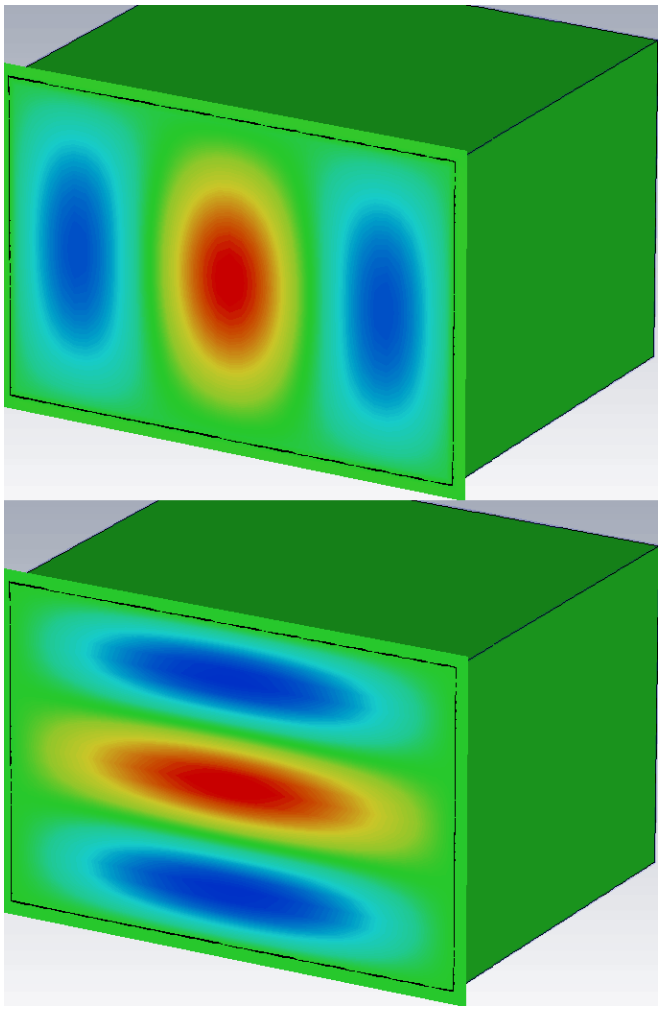

FIG. 4. Field strengths at one instant in 8×12ft waveguide, excited by 'Field Source' wall currents. Red is most positive field, blue is the most negative field, green is neutral, and coloring is linear. Top: TE31 mode shown at $\sim$ 137.46MHz (shown at 135MHz). Bot: TE13 mode shown at $\sim$ 188.92MHz (shown at 190MHz).

To verify this excitation method, the room modes are found and compared to predictions. In a conducting box of interior dimensions $a \times b \times d$, Maxwell's equations predict resonances at frequencies[9]:

$$\omega_{mnp} = c\pi\sqrt{\left(\frac{m}{a}\right)^2 + \left(\frac{n}{b}\right)^2 + \left(\frac{p}{d}\right)^2}. \tag{12}$$

The modes in a waveguide are just those in a conducting box with $d \to \infty$. For example, a 8×12ft waveguide has modes $\omega_{31} = 137.46$MHz and $\omega_{31} = 188.92$MHz. Exciting current at these frequencies shows the desired modes (see figure 4), providing evidence that the excitation is working as expected. Other modes were verified.

These currents are used to determine the (effective) antenna factor of an antenna in our room. Since $AF(\nu) = |E(\nu)/V(\nu)|$ and the voltage is measured, the equivalent field strength also must be found to determine the antenna factor. This field strength is that which would cause these currents in vacuum - it is not the field in the resonating Faraday cage. On resonance, the field in the room is increased; off resonance and at large wavelengths (those larger than the waveguide), the field in the room is suppressed due to the requirement of $E_{\|} = 0$.

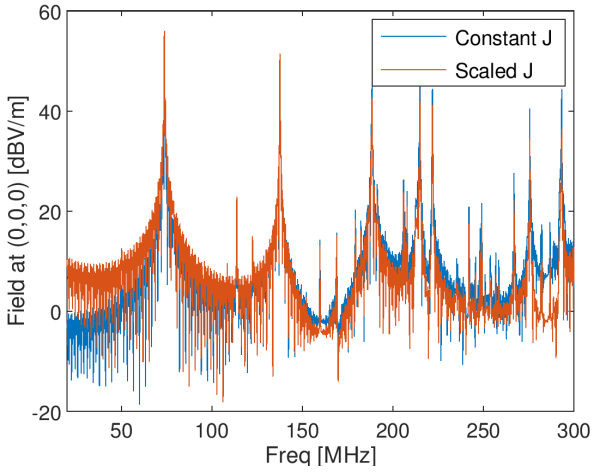

FIG. 5. Absolute value of electric field at the origin of the room (figure 2) when excited by wall currents of constant strength across the frequency range (blue) and when the currents are scaled by frequency (equation 13). Room modes are visible as the peaks in field strength.

To circumvent this problem, the field at the origin of the room is simulated across the frequency range of interest and is manually chosen at a high frequency away from resonances ($\nu_0 \approx 285$MHz), with field $E \approx 1.2$V/m. The current at all frequencies is then scaled to:

$$J(\nu) = k\frac{J_0(\nu_0)}{E(\nu_0)\nu} \approx k\frac{1}{1.2\nu}, \tag{13}$$

where k fixes units, $J_0(\nu_0)$ is the original current density (arbitrarily chosen) exciting fields at ν_0, $E(\nu_0)$ is the field at the origin at that frequency, and $J(\nu)$ is the corrected driving current at ν. This scaling should (relatively) increase the electric field strength at low frequencies, which is verified in the simulations of the room modes in the detailed room model (see figures 5 and 2). These currents, then, are equivalent to a 1 V/m field at the origin, allowing the antenna factor to be calculated: $AF(\nu) = 1\text{V/m}/|V(\nu)|$.

B. Experiment Modeling

The experiment is modeled in Autodesk Inventor and simulated in CST. There are three sections of the modeling. The room needs to be modeled (see figure 2), the antenna needs to be modeled (see figure 7), and the electrical components of the antenna need to be modeled (see figure 3).

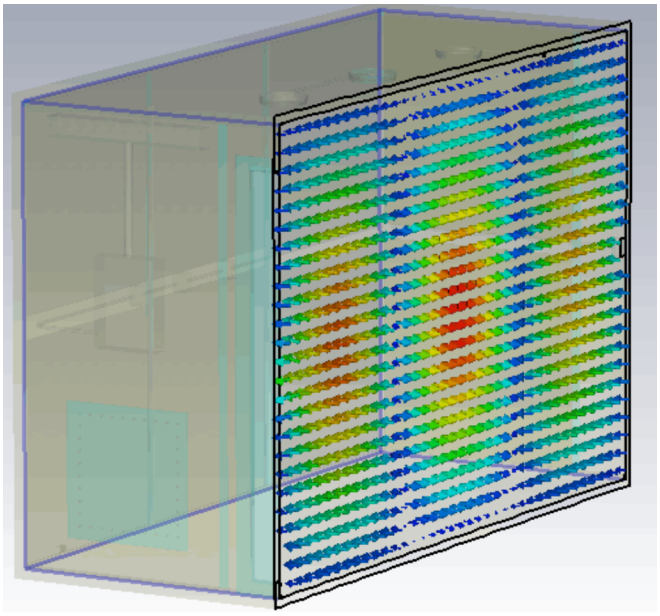

FIG. 6. Field strengths at one instant in $8 \times 10 \times 12$ft Faraday cage, excited by 135MHz 'Field Source' wall currents. Red is most positive field, blue is the most negative field, green is neutral, and coloring is linear. This shows the TE310 mode which is expected at ~ 137.46MHz in the $8 \times 10 \times 12$ft room.

1. *Room Modeling*

The experiment is in a $8 \times 10 \times 12$ft Faraday cage to block background electromagnetic fields. The inside of this cage is complicated and features must be modeled to get an accurate antenna factor result.

In the frequency range of current interest ($30 \rightarrow 300$MHz), conductors of size $\lambda_{\min}/4 \approx 0.25$m or larger act as antennae and thus will have large effects on results. For example, the 2x3 array of lights at the roof of the room of diameter 0.25m strongly affect results. Similarly, the door handle is of length ~ 0.7m and must be modeled carefully. Finer details were also modeled.

As a first-pass verification, the room modes in this detailed model were found. While the details will modify the exact resonant frequencies, they should be similar to that of a $8 \times 10 \times 12$ft resonating cavity, which is what is found (see figure 6; other frequencies were investigated).

These simulations should also be done for the room with smaller features excluded (smaller than $\lambda_{\min}/4$). Smaller features are excluded in some simulations so that the mesh resolution can be decreased, allowing for faster simulations. These features should have minimal effects on the results, but this should be verified by simulating the room modes for the room with the features excluded and comparing fields side-by-side.

While room modes were simulated, more time should be spent in physically measuring the room modes and verifying that the simulations show the same modes. This may include additions of more complicated features in the room (e.g., batteries, wires, another antenna).

C. Antenna Modeling - Electrical

For AC circuits much larger than the wavelength of the electrical signal, currents may be thought to flow instantaneously. For high frequencies, the wavelength of the signal is on the same order of magnitude as the size of the circuit and wave effects must be taken into account.

A well studied phenomenon is the reflection of signals when they reach an impedance boundary (every conductor can be modeled as resistors, inductors, and capacitors; some conductor geometries have higher impedances than others). This effect is typically undesired as it can lead to standing waves and harder to detect signals, as the signals are not being transmitted.

For example, the voltage standing wave ratio (VSWR) is the ratio of the maximum voltage amplitude to the minimum voltage amplitude anywhere on an antenna. If there were no reflection at the feed, the VSWR would be 1. Reflection at the feed, raises the VSWR and is undesirable.

To fix this issue, electrical circuits are used to minimize/reduce the impedance mismatch. These circuits are called baluns and they are crucial to effective antenna designs. The simplest balun is just a voltage transformer, but designs can also become very complicated.

In this experiment, the electrical aspect of the circuit is expected to be a voltage transformer (see figure 3), but inability to open the antenna due to warranties prevents further determination of balun details. Fortunately, the electrical aspect of this circuit can be (roughly) simulated by manually setting the input impedance to the simulated antenna. This will lose some fine details, but at this stage it is OK and those finer details would require an accurate balun model and opening of the antenna.

D. Antenna Modeling - Physical

The physical modeling of the antenna is also important since that affects the antenna factor. Manufacturer 3D models are not available so hand measurements were made and used to generate a 3D model (see figure 7).

Some geometric details of this antenna are unknown as the antenna is sealed and cannot be opened. These details affect the impedance of the antenna and are estimated. For example, at the bottom of the antenna are two parallel conductors (a transmission line). The radius of these conductors, their spacing, the length, and more are all unknowns.

The free-space antenna factor is provided by the manufacturer and can be used to gain confidence in the 3D model. Iterations of modifying unknown antenna geometry, simulating the antenna factor, and comparison to the given antenna factor were done until the shown

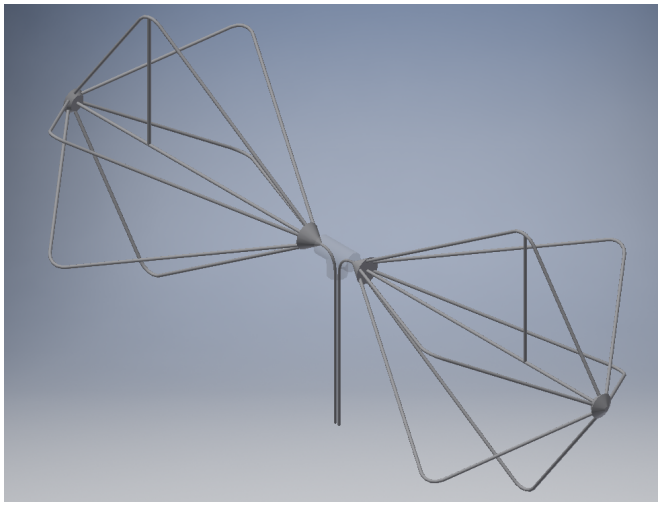

FIG. 7. CAD model of 30 → 300MHz bicon antenna currently being used in the dark radio experiment.

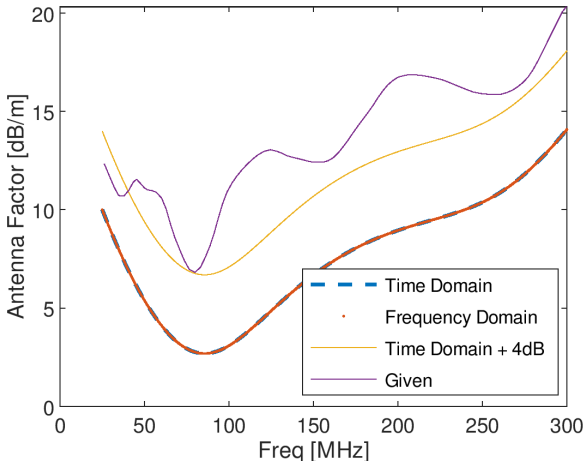

FIG. 8. Simulated antenna factor of the CAD bicon antenna (figure 7) compared to the reported value (purple). The simulated antenna factor shows the same rough shape, but is offset by approximately 3dB from the given antenna factor. This is likely due to characteristics of the electric circuit not being included and is currently being investigated. The agreement between the time domain solver and the frequency domain solver (fundamentally different processes) provides good evidence that simulation instability is not a current worry.

model with the following antenna factor (see figure 8) were found.

There are discrepancies between the manufacturer antenna factor and the simulations, but these are currently finer details to be fixed in the future with a more-detailed antenna model.

E. Antenna Factor Simulations

The final step in these simulations is to place the antenna inside the detailed room with the 'Field Source' excitation running as described in section IV A, and to measure to feed voltage. Running time-domain simulations at -15dB accuracy with a simplified room model (fine details excluded), frequency range of 30-300MHz, 25 mesh cells per wavelength, with a bicon (4mm transmission line gap; 12.5625in transmission line length) in the room results in antenna factor in figure 9. This antenna factor is noisy, but noise is expected from the detailed geometry in the room. Investigation should be done, however, to determine what peaks are from simulation errors/instability, and what peaks are real.

These simulations were surprisingly quick (less than 1day) and thus the accuracy and mesh resolution can be increased for improved results. Additionally finer features may also be included. These changes are to identify any possible simulation instabilities giving faulty results.

Another approach to gain confidence in these results is to simulate the same scenario with the frequency domain solver (fundamentally different solution method). This solver is less developed by CST and less benchmarking has been done with it at UC Davis because it is unable to do some simulations of interest, but it should give similar results to the time domain solver.

V. CONCLUSION

To determine the (effective) antenna factor, a relationship between field strength and feed voltage that would give the coupling ϵ of the dark field, CST simulations are performed. When/if a signal is measured with the physical experiment, the simulated antenna factor will give ϵ.

These simulations are complicated, requiring accurate models of the antenna, room, and fields. All of these steps have been modeled and verified, albeit more verification of all of these steps is greatly desired. Another point of verification is in the final, antenna factor, simulation. The resolution and accuracy of this simulation may be increased to see how the structure of the antenna factor varies, to determine what of the structure is due to simulation error and what is real. The goal of these modifications is to gain confidence in the antenna factor prediction.

VI. ACKNOWLEDGMENTS

I would like to thank Dr. Tony Tyson for his guidance and encouragement throughout the summer. I would also like to thank Dr. Mani Tripathi for being a great mentor in reminding me of important parts in science that are more easily forgotten, like communicating your work with others. I would also like to thank Dr. Rena Zieve and the

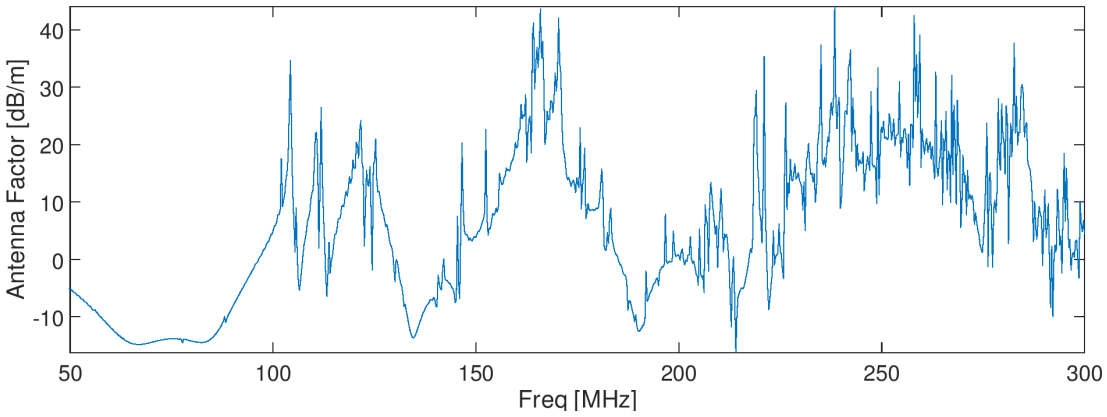

FIG. 9. Simulated antenna factor of the CAD bicon antenna placed inside the Faraday cage with small details excluded.

NSF for making this opportunity happen. Lastly, I would like to thank Dr. Ragnar Stroberg for not only teaching me the necessary field theory to understand dark photons, but also being one of my best professors/mentors.

[1] D. S. Akerib et al. LUX-ZEPLIN (LZ) Conceptual Design Report. 2015.

[2] Jo Bovy and Scott Tremaine. On the local dark matter density. *Astrophys. J.*, 756:89, 2012. doi:10.1088/0004-637X/756/1/89.

[3] Saptarshi Chaudhuri, Peter W. Graham, Kent Irwin, Jeremy Mardon, Surjeet Rajendran, and Yue Zhao. Radio for hidden-photon dark matter detection. *Phys. Rev.*, D92(7):075012, 2015. doi:10.1103/PhysRevD.92.075012.

[4] Saptarshi Chaudhuri, Kent Irwin, Peter W. Graham, and Jeremy Mardon. Fundamental Limits of Electromagnetic Axion and Hidden-Photon Dark Matter Searches: Part I - The Quantum Limit. 2018.

[5] Benoit Famaey and Stacy McGaugh. Modified Newtonian Dynamics (MOND): Observational Phenomenology and Relativistic Extensions. *Living Rev. Rel.*, 15:10, 2012. doi:10.12942/lrr-2012-10.

[6] J. L. Feng et al. Planning the Future of U.S. Particle Physics (Snowmass 2013): Chapter 4: Cosmic Frontier. In *Proceedings, 2013 Community Summer Study on the Future of U.S. Particle Physics: Snowmass on the Mississippi (CSS2013): Minneapolis, MN, USA, July 29-August 6, 2013*, 2014. URL `https://inspirehep.net/record/1278570/files/arXiv:1401.6085.pdf`.

[7] David S. Graff and Katherine Freese. Analysis of a hubble space telescope search for red dwarfs: limits on baryonic matter in the galactic halo. *Astrophys. J.*, 456:L49, 1996. doi:10.1086/309850.

[8] Peter W. Graham, Jeremy Mardon, Surjeet Rajendran, and Yue Zhao. Parametrically enhanced hidden photon search. *Phys. Rev.*, D90(7):075017, 2014. doi:10.1103/PhysRevD.90.075017.

[9] David J Griffiths. *Introduction to electrodynamics; 4th ed.* Pearson, Boston, MA, 2013. URL `https://cds.cern.ch/record/1492149`. Re-published by Cambridge University Press in 2017.

[10] Joerg Jaeckel and Andreas Ringwald. The Low-Energy Frontier of Particle Physics. *Ann. Rev. Nucl. Part. Sci.*, 60:405–437, 2010. doi:10.1146/annurev.nucl.012809.104433.

[11] Lord Kelvin. Baltimore lectures on molecular dynamics and the wave theory of light, 1904.

[12] R. W. P. King, T. T. Wu, and L. . Shen. The horizontal wire antenna over a conducting or dielectric half space: Current and admittance. *Radio Science*, 9(7):701–709, July 1974. ISSN 1944-799X. doi:10.1029/RS009i007p00701.

[13] S. S. McGaugh, F. Lelli, and J. M. Schombert. Radial Acceleration Relation in Rotationally Supported Galaxies. *Physical Review Letters*, 117(20):201101, November 2016. doi:10.1103/PhysRevLett.117.201101.

[14] Note1. Since only massless particles travel at the speed of light, dark photons travel at speeds less than c.

[15] Note2. The word 'bound' is crucial. Were dark photons not massive, then they could not be bound (except by black holes) and thus they could not be a dark matter candidate.

[16] Note3. When the Lagrangian and Hamiltonian densities contain no explicit time dependence, which is the case here.

[17] Note4. For example, the Yagi antenna is a collection of dipole antennae in close proximity. It has different characteristics than a dipole antenna. Other examples like antenna near conductors have also been studied[12].

[18] Note5. 'Effective' indicates that the surroundings are being considered. Also referred to as 'in situ'.

[19] Note6. A good question is how do we include gravity into this Lagrangian since we know that light is bound by black holes and the dark photons can be bound. This is captured in modifications of the metric from $(-,+,+,+)$ to more complicated tensors.

Appendix A: Variables and Conventions

1. Conventions

SI units are used throughout this writeup due to the familiarity of the equations, even if the equations can be made cleaner by clever unit choices. The metric is set to be $(-,+,+,+)$ throughout the whole writeup.

In equation 2, magnetic charges are included with the convention of magnetic charge units being A·m. After that equation, we assume $\rho_m = 0$ and $\mathbf{j}_m = 0$ since there has been no evidence for magnetic charges.

2. Variables

Any variable with an apostrophe ' is dark. For example, while A_μ is the 'standard' four-potential, A'_μ is the dark four-potential. We will only list 'standard' variables below

TABLE I. Variables

Symbol	Name	Definition
$\mathbf{A}$	vector potential	equation B9
A^μ	four-potential (diagonalized)	linear combinations of a^μ and a'^μ[8]
a^μ	four-potential	$a^\mu = (V/c, \mathbf{A})$
$\Box$	d'Alembert operator	$\Box = \partial_\mu \partial^\mu = -\partial^2/(c\partial t)^2 + \nabla^2$
$\mathbf{B}$	magnetic field	N/A
∂_μ	four-gradient	$\partial_\mu = (\partial/\partial(ct), \nabla)$
$\mathbf{E}$	electric field	N/A
$\epsilon_{i_1 i_2 i_3 i_4}$	4D Levi-Civita symbol	$\epsilon_{i_1 i_2 i_3 i_4} = 0$ if $i_a = i_b$ for any $a \neq b$ otherwise $\epsilon_{i_1 i_2 i_3 i_4} = (-1)^{\text{permutation parity}}$
$f^{\mu\nu}$	field-tensor	$f^{\mu\nu} = \partial^\mu a^\nu - \partial^\nu a^\mu$
$F^{\mu\nu}$	field-tensor (diagonalized)	$F^{\mu\nu} = \partial^\mu A^\nu - \partial^\nu A^\mu$
$G^{\mu\nu}$	dual field-tensor	$G_{\mu\nu} = \epsilon_{\alpha\beta\mu\nu} F^{\alpha\beta}/2$
J^μ	four-current	$J_\mu = (c\rho_e, \mathbf{j}_e)$
$\mathbf{j}_e$	electric current density	continuity equation $\nabla \cdot \mathbf{j}_e = -\partial\rho_e/\partial t$ also called $\mathbf{j}_e = \mathbf{j}$
$\mathbf{j}_m$	magnetic current density	magnetic continuity equation $\nabla \cdot \mathbf{j}_m = -\partial\rho_m/\partial t$
$\mathcal{L}$	Lagrangian density	$L = \int \mathcal{L} d\text{Volume}$
L	Lagrangian	N/A
p^μ	four-momentum	$p^\mu = m v^\mu$
Q_e	electric charge	also called $Q_e = q$
Q_m	magnetic charge	N/A
ρ_e	electric charge density	$\rho_e = dQ_e/d\text{Volume}$ also called $\rho_e = \rho$
ρ_m	magnetic charge density	$\rho_m = dQ_m/d\text{Volume}$
τ	proper time	time between events in frame which they occur in same place
V	voltage	equation B9
v^μ	four-velocity	$dx^\mu/d\tau$
x^μ	four-position	$(ct, \mathbf{r})$

3. Dark Matter Survey

The motivation for dark matter is: observable mass distributions (stars, planets, etc.) give predictions differing from astronomical observations. A modern example of this discrepancy is the galactic rotation curve: stably orbiting objects travel at linear velocities increasing with mass enclosed and decreasing with distance from orbit center. Measurements of linear velocities are higher than expectations at large radii, implying that either our law of gravitation is wrong or that there is unobserved mass in galaxies at large radii.

There is a zoo of potential dark matter theories (see 10) but, luckily, many experiments searching for one candidate can rule out other candidates at the same time. The most prevalent candidates are MACHOs, WIMPs, and axions,

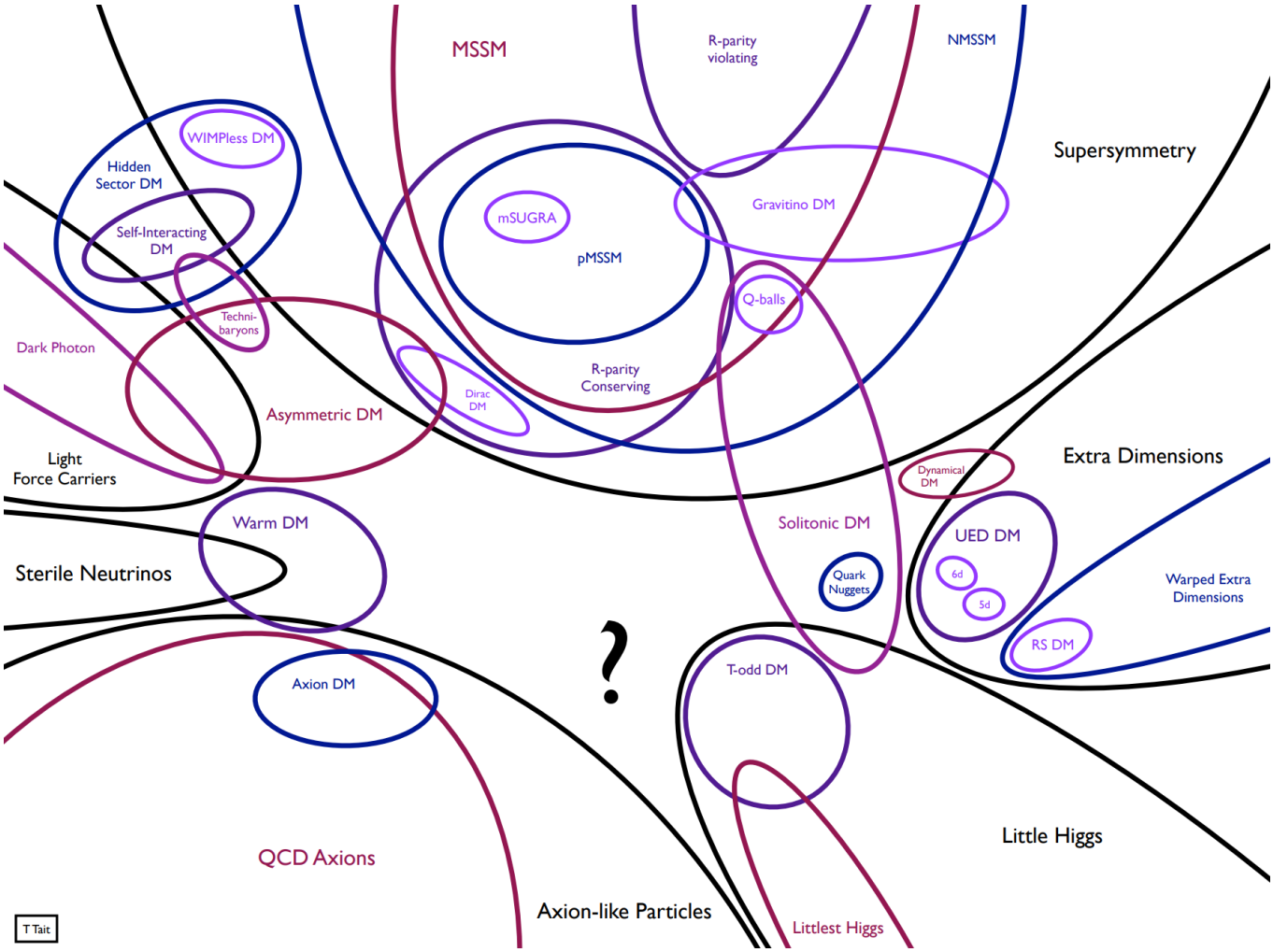

FIG. 10. (taken from [6]) Dark matter zoo of possibly theories.

but other theories such as dark photons are also promising. Incorrect dynamics, also, could explain this discrepancy and not require dark matter. Given the extended search for dark matter and null results, modified dynamics should also be taken seriously.

a. Dynamics/Gravitation

A theory (Modified Newtonian Dynamics or MoND[5]) generated to account for this discrepancy is that our laws of dynamics are flawed for low accelerations. Since most experiments are done on solar system length scales (or smaller) with high accelerations, deviations from our law of gravitation could have gone unnoticed. With increased observations on large length scales (galaxies and larger), modifications of the dynamics can be tested. While such modifications can match some observations (e.g., galaxy rotation curves), none so far have been able to match all astronomical observations (e.g., galaxy cluster dynamics), making MoND not-promising. There has recently been evidence[13] making MoND more viable, but many questions are unanswered.

b. MACHOs and WIMPs

Theorems have been generated that posit undetected mass ('dark matter') to account for the discrepancies. One of these such theorems is that of massive compact halo objects (MACHOs), positing matter (planets, dim stars, black holes) throughout the universe that does not emit light and thus is difficult to detect. This theory of dark

matter is attractive because it does not require new physics, just improved observations. Gravitational lensing observation, however, find that MACHO concentrations cannot explain dark matter[7], and thus other theorems must be investigated.

The arguably most prevalent dark matter theory is currently that of weakly interacting massive particles (WIMPs). This theory is a consequence of supersymmetry and it posits new physics, stating that there are (relatively heavy) massive particles everywhere in this universe but that only weakly interact with familiar matter and thus have not been yet noticed.

Despite many experiments at CERN and throughout the world, no detections of these particles has yet been made, ruling out much of the parameter space. Some cutting edge experiments, for example, search for this dark matter through looking for light flashes in large vats of liquid (similar to Super-Kamiokande's investigation of neutrinos). One of these such experiments is the LZ experiment at the Sanford Underground Research Facility[1]. These new experiments can explore more and more parameter space, but the lack of results in previous generations reduces the parameter space for WIMPs, making them less and less likely as a dark matter candidate.

Appendix B: Field Theory

1. Lagrangians

Light is a traveling excitation of electric and magnetic fields. It, along with the rest of electromagnetism, is fully described by Maxwell's equations (see equation 2). Work is simplified in covariant notation in which Maxwell's equations become

$$\begin{aligned} \partial_\nu F^{\mu\nu} &= \mu_0 J^\mu \\ \partial_\nu G^{\mu\nu} &= 0. \end{aligned} \tag{B1}$$

This can be further abstracted with by introducing a Lagrangian density $\mathcal{L}$:

$$\mathcal{L} = -\frac{1}{4\mu_0} f_{\mu\nu} f^{\mu\nu} + a_\mu J^\mu \tag{B2}$$

which gives equation B1 from extremizing the action (using the Euler-Lagrange equation) [19].

We are interested in modifications of Maxwell's equations by adding 'dark' fields $f'_{\mu\nu}$ which come with a 'dark' vector potential a'_μ. These are analogous to the standard electric/magnetic fields $f_{\mu\nu}$ and the standard vector potential a_μ except the dark counterparts are massive with mass m. These dark fields interact with the 'standard' fields through a coupling ϵ[8]:

$$\mathcal{L} = -\frac{1}{4\mu_0}(f_{\mu\nu} f^{\mu\nu} + f'_{\mu\nu} f'^{\mu\nu} - 2\epsilon f_{\mu\nu} f'^{\mu\nu}) + \frac{1}{2\mu_0} m^2 a'_\mu a'^\mu + a_\mu J^\mu. \tag{B3}$$

Specifically, the dark fields are an inclusion of a new U(1) gauge symmetry (effectively stating that physics is invariant of the phase of the wavefunctions) and the connection between the dark fields with standard fields is called kinetic mixing, where ϵ is the strength of this mixing.

We can define A_μ and A'_μ as linear combinations of a_μ and a'_μ so as to simplify this Lagrangian ('diagonalizing' it), giving

$$\mathcal{L} = -\frac{1}{4\mu_0}(F_{\mu\nu} F^{\mu\nu} + F'_{\mu\nu} F'^{\mu\nu}) + \frac{1}{2\mu_0} m^2 A'_\mu A'^\mu + (A_\mu + \epsilon A'_\mu) J^\mu. \tag{B4}$$

2. Equations of Motion

Treating each component of A_μ and of A'_μ as an independent field, we extremize the action to get the equations of motion. That is, we evaluate:

$$\frac{\partial \mathcal{L}}{\partial A_\mu} - \partial_\nu \left(\frac{\partial \mathcal{L}}{\partial(\partial_\nu A_\mu)} \right) = 0 \tag{B5}$$

and

$$\frac{\partial \mathcal{L}}{\partial A'_\mu} - \partial_\nu \left(\frac{\partial \mathcal{L}}{\partial(\partial_\nu A'_\mu)} \right) = 0. \tag{B6}$$

We do not perform such a calculation in detail because we do not need to. This is because, in this diagonalized Lagrangian, the terms with A_μ or $\partial_\nu A_\mu$ look like those in equation B2. Since equation B2 is the Lagrangian that gives Maxwell's equations, we also get Maxwell's equations for the A_μ terms:

$$\partial_\nu F^{\mu\nu} - \mu_0 J^\mu = 0 \tag{B7}$$

The terms with A'_μ or $\partial_\nu A'_\mu$ also look like equation B2, except J^μ is replaced with ϵJ^μ and there is an additional term $m^2 A'_\mu A'^\mu/2$. This additional term just adds $m^2 A'^\mu$ to the Euler-Lagrange equation and thus results in:

$$\partial_\nu F'^{\mu\nu} - \epsilon(\mu_0 J^\mu) + m^2 A'^\mu = 0. \tag{B8}$$

3. Proca Equations

Maxwell's equations (and their dark counterpart) directly follow from equations B7 and B8 along with the implicit definition of the four-potential A as:

$$\begin{aligned} \mathbf{E} &= -\nabla V - \frac{\partial \mathbf{A}}{\partial t} \\ \mathbf{B} &= \nabla \times \mathbf{A}. \end{aligned} \tag{B9}$$

We do not write out Maxwell's equations in the standard form (equation 2), however, since the mass term in equation B8 makes potential formulation more natural. This potential formulation follows from the four-potential definition of the field tensor:

$$F^{\mu\nu} = \partial^\mu A^\nu - \partial^\nu A^\mu \tag{B10}$$

and identical for the dark version. Plugging this in and choosing the Lorentz gauge:

$$\partial_\nu A^\nu = 0, \tag{B11}$$

we get equations 1 and 3 which are two copies of the Proca equation. The Proca equation is effectively a generalization of Maxwell's equations, allowing $m \neq 0$.

By considering the Lagrangian of a charged particle in the standard and dark fields:

$$\mathcal{L} = \frac{1}{2} m v_\mu v^\mu + q(A_\mu + \epsilon A'_\mu) v^\mu, \tag{B12}$$

we get the Lorentz force law by extremizing the action:

$$\frac{dp^\mu}{d\tau} = q(F^{\mu\nu} + \epsilon F'^{\mu\nu}) v_\nu. \tag{B13}$$

This law shows the direct consequences of the inclusion of a dark field: there will be forces on charged objects by the dark fields after a suppression of ϵ.